GPS Multipath Detection and Exclusion with Elevation-Enhanced Maps

Carolina Piñana-Diaz, Rafael Toledo-Moreo, David Bétaille, Antonio F Gómez-Skarmeta

GPS Multipath Detection and Exclusion with Elevation-Enhanced Maps

Carolina Piñana-Diaz, Rafael Toledo-Moreo, IEEE Member
David Bétaille, IEEE Member, Antonio F. Gómez-Skarmeta

***Abstract*— The reflections of satellite signals in the environment of Global Positioning Systems (GPS) receivers cause significant errors in their position estimates. Particularly critical are the errors due to the so called non-line-of-sight (NLOS) satellites. In a NLOS situation, the only way the satellite signal reaches the receiver is by means of reflections on plane surfaces, typically buildings, causing overestimates of the pseudoranges between the satellites and the antenna. Receivers not always distinguish between the direct signals and the multipath effects, leading to un-modelled GPS errors. This paper presents a solution to the problem of multipath effects in urban areas, by means of simple elevation models of the environment. The description of the buildings is stored in a elevation-enhanced digital map (EEMap) that can be consulted to decide whether a certain satellite may be in direct view or not. The validity of the concept is proven by means of real experiments in built-up areas of Spain.**

I. INTRODUCTION

Global Navigation Satellite Systems (GNSS) are well known as the most suitable technology for vehicular global positioning. GNSS are satisfactory applied in a number of fields related to intelligent transportation systems (ITS) and intelligent vehicles, such as fleet management or in-car navigation [1], [2]. However, at the moment GNSS lacks the necessary accuracy and reliability to be applied in more challenging missions, such as lane-level positioning or collision avoidance applications [3]. The main drawbacks of commercial GNSS are lack of coverage in certain scenarios, such as tunnels, covered parking lots and urban canyons, lack of accuracy for precision applications, such as lane level guidance, and lack of integrity in the solution due to un-modelled errors. It is expected that the increase of satellites in view coming from different constellations such as North-American Navstar GPS (Global Positioning System), the Russian Glonass (Global Navigation Satellite System) and the European Galileo may raise the final coverage of GNSS. However, there will be scenarios where more satellites in the sky will not help, such as parking lots of multiple stories, etc., and aiding sensors are needed. The GNSS inaccuracies are now smaller than ten years ago [4] thanks to the upgrades in satellites and receivers. Double frequency receivers show very good precision but their prices must decrease before being applicable in the vehicular domain. Finally, the appearance of un-modelled errors due to strong assumptions such as one fault at one time at the user-end, or Gaussian distributions models for GNSS errors is a clear showstopper for safety and liability critical applications of the GNSS for vehicles [7], [5], [9]. Among all possible un-modelled errors, the most challenging is the multipath propagation of the satellite signals in the environment of the receiver [3].

Multipath can be classified as line-of-sight (LOS), when the receiver collects both the direct and the reflected signals, and non-line-of-sight (NLOS), when there is no direct view of the satellite and only the reflected signal is acquired. Current receivers are quite good at separating the original signal from the reflected one in the LOS case, but not so much for NLOS. Fig. 1 depicts a NLOS scenario. The blue arrows represent the bounds of GNSS satellite visibility caused by the buildings, and the line of visibility between the antenna and the satellites is shown with black dashes. In this image, satellites 1 and 2 are in direct view, but satellite 3 is not, and the signal arrives at the antenna exclusively due to the reflection on a building. With one more satellite or an assumption such as altitude-hold respect to the previous position, the vehicle position can be calculated. However, the value of the satellite 3 pseudorange is larger than it should, causing significant errors in the final estimate of the vehicle position.

Our approach to solve this problem is based on the fact that most of the multipath effects are due to the reflections in buildings around the vehicle environment. An elevation-enhanced map (EEMap) of the buildings can be understood as a visibility map of the GPS satellites in flight that can inform whether or not a satellite is in direct view from a given location. If despite the fact that there is no direct view the signal arrives at the receiver, it is assumed that it is as a consequence of multipath reflections and the pseudorange measurement is discarded. Furthermore, if the satellite configuration resulting of disregarding the space vehicles in NLOS presents a bad geometry with a poor value of Dilution Of Precision (DOP), the solution is also labelled as unreliable.

The rest of the paper is organized as follows: our EEMaps are introduced in Section II; the positioning algorithms are

This work has been supported by the Spanish Ministry of Transportation and Ministry of Science and Innovation under the projects SATELITES (FOM/2454/2007) and SEISCIENTOS (TIN2008-06441-C02), respectively, and it has been carried out inside the Intelligent Systems and Telematics group of the University of Murcia, awarded as an excellence researching group in frames of the Spanish Plan de Ciencia y Tecnología de la Región de Murcia (04552/GERM/06).

Carolina Piñana-Diaz, Rafael Toledo-Moreo and Antonio F. Gómez-Skarmeta are with Department of Information and Communication Engineering, Faculty of Computer Science, University of Murcia, 30100 Murcia, Spain. Rafael Toledo-Moreo is also with the Department of Electronics and Computer Technology, Technical University of Cartagena, Spain. David Bétaille is with IFSTTAR (French Institute of Sciences and Technology for Transport, Development and Networks) Nantes, France. carolina.pinana@um.es, toledo@um.es, david.betaille@ifsttar.fr, skarmeta@um.es

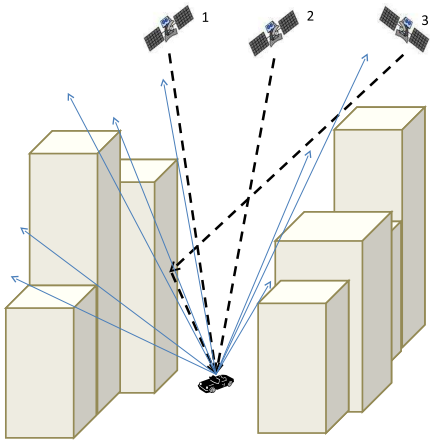

Fig. 1. Scenario with NLOS multipath.

described in Section III; Section IV presents briefly how the DOP concept is applied to our method. In Section V field tests prove the validity of our concept; finally, main conclusions are drawn in Section VI.

II. EEMAPS

Following the line of the European CVIS project [8], where enhanced maps (Emaps) are developed to improve the quality of the vehicle positioning, our approach aims at avoiding multipath by exploiting the information stored in digital maps regarding building locations and sizes. Buildings are the elements that contribute more remarkably to multipath effects, particularly in the cities. For that reason, for the moment our solution only includes buildings. Bridges can also be taken into account in this approach since they can be described as roads segments in the frame of an Emap, as presented in [6], but they are out of the scope of this paper. Although trees also cause disruptions in the GNSS signals, in urban environments its impact is much less significant.

A. Building model

In the process of elevation map modelling, building modelling is the key to identify the necessary information to reliably represent buildings.

In this work the World Geodesic System of 1984 (WGS-84) coordinate, which is the same coordinate used by the GPS receiver, was selected as the coordinate to build the elevation map. Further conversions into Earth-Centered Earth-Fixed (ECEF) frame will be performed to compute user position and determine satellite visibility in urban areas. For each building, latitude and longitude values of the two corners nearest to the road are stored, as well as its width and height. The description of the buildings follows the format given in Table I, where subscripts 1 and 2 stand for the 2D position ends of the facade under consideration (represented as the ends of each red segment in Fig. 2).

B. Extraction of building features

Two methods for extracting the model parameters of the buildings presented in Table I were developed, and are

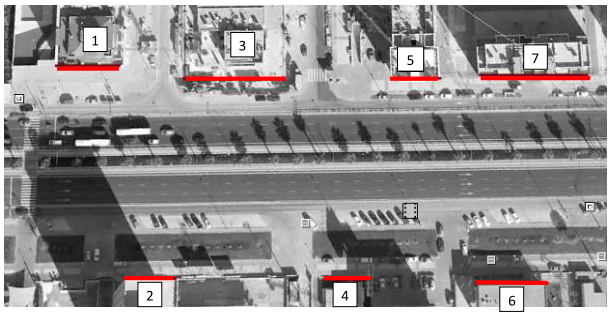

Fig. 2. Aerial view of an urban scenario with modelled buildings in Murcia, Spain.

presented in the next sections. First method, named "Building Image-based Method", depends on the complete visibility of the building. Building images are obtained from Google Earth using the Street Viewer tool. This allows fast prototyping, avoiding extensive field campaigns for extracting the building features. However, since the complete view of the building is not always available, a second method named "Story-based Method" based on the number of stories is proposed. It consists in applying the same art as the "Building Image-based Method" in images that only show isolated parts of buildings, such as the ground or the first floor, something common in urban canyons. Finally, a comparison of both methods shows the consistency of our approach.

1) Building Image-based Method: A dedicated algorithm based on Google Earth images processing is proposed for simply and efficiently obtaining building heights. The first step employs a frontal view of the building facade provided by the Street Viewer tool of Google Earth. Then, a Canny detector algorithm [10] is implemented to get an edge intensity image. The small-scale model obtained with the low-level detector provides edge information of the scene which is used to calculate the relationship between the width and the height of the building. Since its real width can be measured in the aerial image provided by Google Earth (Fig. 2) it is possible to extrapolate feature information to calculate the real height of the building. Fig. 3.a) shows a frontal view of a building located in the street Avenida Juan Carlos I of Murcia, Spain. Its respective edge detected image is depicted in Fig. 3.b).

Experimental results show that the proposed algorithm works well on cases in which a complete frontal view of the building is available in the Street Viewer tool of Google Earth.

2) Story-based Method: An entire view of the facade of the building is not often available in Google Earth, especially in narrow streets with limited visibility where the only visible features correspond to the ground and first floors. In these

TABLE I
BUILDING MODEL PARAMETERS.

Bldg Id	Lat_1	Lon_1	Lat_2	Lon_2	w	h

a) b)

Fig. 3. a) Frontal view of a building for feature extraction. b) Edge intensity image after applying the Canny algorithm.

cases, it is possible to use the prior algorithm to detect edges only of available parts and then extrapolate measurements to the whole building just by counting the number of stories. Given that the height of all the stories in a building is the same, by applying this technique the height of the entire building can be computed as follows:

$$h = k_1 \times s + k_2$$

where s denotes the number of stories, k_1 represents a constant value of the height of an arbitrary floor and k_2 is the height of the ground floor along with any extra element not included in a standard story of the building. Both parameters are obtained with the Canny detector estimation method.

3) Comparison: To validate this algorithm a comparison between the building-image and story-based methods has been performed. Both techniques have been used to calculate heights of a subset of buildings located in Murcia, Spain. Results are given in Table II. As it can be seen, the difference between heights computed using one or another method is only slightly different, with a median error percentage of 0.48%, and the methods show consistency. Additionally, these values can be compared with real values given by certain buildings with good results. A precise determination of the relative height errors based on precise elevation models and building databases is under progress. Nevertheless, the inaccuracies caused by the measurement tools of Google Earth are taken into account in the algorithm for determining the satellites in line-of-sight. As it will be shown, these building models presented in this section will be a powerful tool in order to decide whether a certain satellite may be in direct view or not.

TABLE II

COMPARISON OF BUILDING HEIGHT ESTIMATES.

Bldg Id	Method 1	Method 2	Relative Error
1	26.27	26.36	0.0034
2	38.99	38.70	0.0074
3	26.65	26.85	0.0075
4	25.07	25.01	0.0025
5	19.92	19.98	0.0033

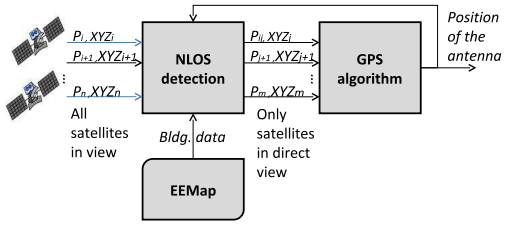

Fig. 4. Flowchart scheme of the positioning process.

III. POSITIONING ALGORITHM

This Section describes the algorithms developed for verifying the goodness of the concept introduced in the paper. In Fig. 4 a flowchart shows schematically the steps followed to provide multipath free positions.

First, the algorithm that detects whether a satellite is in LOS or in NLOS, called from now on the NLOS detection algorithm, is applied (Section III-A). Inputs of that process are the satellite measurements, the EEMap, and an estimate of the vehicle position obtained for instance from a simple extended Kalman filter. NLOS satellites are discarded, and only satellites in LOS are used as inputs of the second step, the GPS problem solving algorithm, that provides the position of the antenna. For this step, two different approaches are developed: the most common Least Squares (LS) algorithm (Section III-B), and the Bancroft approach (Section III-C). The use of two different positioning algorithms helps avoiding the possible influence of the particularities of a algorithm on the results. In our work both appear to be consistent providing in general similar results.

Let us remark here that ionospheric and tropospheric error corrections are not considered in order to emulate the function of a simple GPS receiver. For the same reason, the Glonass constellation is not exploited.

A. NLOS Detection Algorithm

With the aim of taking into account only satellites in direct view for GPS position calculation, a multipath detection algorithm is proposed for efficiently reject satellites that are in NLOS. See Fig. 1 for a graphic view of the problem.

Since satellite positions can be obtained with the GPS receiver and the coordinates of the corners of the buildings nearest to the road are stored in the EEmap, the following algorithm determines if a satellite signal is received through a direct path. Otherwise the proposed method rejects it.

It is important to note that an initial estimate of the receiver position is required in order to determine satellite visibility in a given area. Let us define $\mathbf{u}_1, \mathbf{u}_2$ as the position vectors from the estimated position of the receiver to both the corners of a given building and $\mathbf{v}$ the vector from the same estimated position of the receiver to a "potentially" visible satellite captured by the receiver.

As that the height of the building has been obtained by the algorithm described in Section II, the interval of non-visibility for a given building can be calculated just

determining the angles between both $\mathbf{u}_1$ and $\mathbf{u}_2$ and $\mathbf{w}$, being $\mathbf{w}$ the imaginary line from the initial estimate of the receiver position and the upper corners of the building.

Once the angles for which a building blocks a path are known, we compute visibility angles for each of the satellites detected by the GPS receiver. As mentioned before, we denote $\mathbf{v}$ the position vector from the initial estimate of the receiver position and satellite $i, \{0 \leq i \leq n\}$, where n corresponds to the total numbers of satellites detected. The interval of visibility for satellite i will be calculated from the angles between $\mathbf{v}$ and the defined above $\mathbf{w}$.

Defining $[\alpha^1, \alpha^2]$ as the interval of occultation of a given building (superscripts 1 and 2 stand for each upper corner) and $[\alpha^1_{sv_i}, \alpha^2_{sv_i}]$ the interval of visibility of satellite i regarding the building:

```
if [α¹_svi, α²_svi] ≤ [α¹, α²]
   then ⇒ Satellite i is in NLOS
else if [α¹_svi, α²_svi] > [α¹, α²]
   then ⇒ Satellite i is in LOS
end
```

NLOS satellites are flagged as not valid for the GPS computation, while those in LOS are accepted. Applying this concept for each building located around the initial estimate of the location of the receiver it is possible to determine visibility of detected satellites along an urban dense area with tall buildings.

B. Least Squares Algorithm

Under the assumption that the pseudorange measured with a GPS receiver, $P_{observed}$, is the sum of a modelled observation, $P_{model} = P_{x,y,z,\tau}$, plus an error term v, it can be written $P_{observed} = P_{x,y,z,\tau} + v$. Applying Taylor's theorem, the residual observation is defined to be the difference between the actual observation and the observation computed using the provisional parameter values:

$$\begin{aligned} \Delta P &\equiv P_{observed} - P_{computed} \\ &= \frac{\partial P}{\partial x}\triangle x + \frac{\partial P}{\partial y}\triangle y + \frac{\partial P}{\partial z}\triangle z + \frac{\partial P}{\partial \tau}\triangle \tau + v \end{aligned} \quad (1)$$

(1) can be written with matrix notation as $\mathbf{b} = \mathbf{A}\mathbf{x} + \mathbf{v}$, which depicts a linear relationship between the residual observations $\mathbf{b}$ and the unknown correction to the parameters $\mathbf{x}$. The column matrix $\mathbf{v}$ contains all the noise terms, which are also unknown at this point. The least squares solution can be found by varying the value of $\mathbf{x}$ until the sum of squares of the estimated residuals, $J(\mathbf{x})$ is minimized. More details of the LS method can be found in [11].

C. Bancroft Algorithm

The direct version of the algorithm Bancroft provides an algebraic and non-iterative solution to the measurement equations. Due to paper length constraints, it is not possible here to include the description of the algorithm. Interested readers can find details in [12].

IV. DILUTION OF PRECISION

Receivers usually provide an estimate of the goodness of the GPS solution based on the geometry of the satellite set employed for calculating the position of antenna. This parameter is named Dilution Of Precision (DOP). Since the elimination of one satellite from the solution generates a new geometry, DOP values given by the receiver must be updated after detecting and removing NLOS satellites. For that reason, a DOP algorithm has been developed and introduced into the decision of whether or not final position is reliable.

A typical DOP threshold value is 10 (DOP has no dimensions and therefore no units are needed), where lower values are good and larger poor. This extra test will serve us well to determine not only if the new configuration of GPS satellites is free of non-line-of-sight multipath, but also if the resulting satellites in view are properly placed in the sky to achieve a good solution. It will be shown that this step is important to obtain good results. Further details about DOP calculations can be found in [13].

V. EXPERIMENTS

The concept introduced in this paper was validated by means of real tests in different urban scenarios in Spain and France. The data were collected by a DGPS receivers and a high-grade inertial navigation system (INS) onboard the vehicles, with the antenna installed on the top of the car. For the tests in Spain, the ground truth reference is obtained in post-processing with a double frequency DGPS. In France, the high-grade INS was employed as a reference for the true trajectory.

A. Field Tests

As it was aforementioned, two sets of experiments were performed. Firstly, experimental trials along a run in a highly masked environment in Murcia, Spain, were performed for proving the concept.

Fig. 5 represents a scenario with a typical situation where some of the satellites used by the receiver for computing GPS position are not in direct view because the nearest buildings block the path. Consequently, position solutions (shown in bottom image) that employ faulty pseudoranges (in red) are far from the ground truth (green), not meeting the GPS specifications. Also the receiver output (cyan), that uses 5 satellites but including one in NLOS, is far from the Bancroft solution calculated with the satellites in LOS (yellow).

Fig. 6 shows the value of the horizontal positioning error (HPE) estimated comparing GPS solutions employing Bancroft along a short period of time in a test performed in Murcia downtown (an image of the test scenario can be seen in Fig. 5.b). Results obtained with the Least Squares algorithm offer similar conclusions and will not be discussed.

Fig. 5. *B*uilt-up scenario where multipath appears. a) Image of the scenario. b) Aerial view: P (green) stands for the ground truth reference; P_{RX} (cyan), the receiver output; P_{NLOS} (red), the two best GPS solutions combining 4 satellites being one in NLOS; P_{DV} (yellow) represents the solution obtained employing the only combination of 4 satellites in direct view (LOS).

During this trajectory, the receiver detected 4 satellites in view during the first 3 seconds. These satellites are identified for the sake of simplicity as 2, 3, 4 and 5. One more satellite, numbered 1, is detected at instant t = 3 s. The proposed NLOS detection algorithm reports that satellite 1 is in NLOS situation, although the receiver did not detect it. For that reason, the receiver output is aberrant, as shown in Fig. 5.a with a cyan circle. On the left side of Fig. 6 are depicted the 4 different GPS solutions calculated using satellite 1 with different symbols and colors. Since the pseudorange value of satellite 1 is erroneous, the consequent position estimates are wrong. The EEMap-based algorithm under consideration informs that the solution obtained employing satellites 2, 3, 4 and 5 is the only one that uses exclusively satellites in LOS, offering consistency in the solution by removing the multipath effects from the GPS output.

Previous tests have shown the concept of the method proposed by the authors. In order to validate this concept more statistical evidences must be shown.

Fig. 7 shows a stretch of a test in a built-up area in Nantes, France. The axis origin have been moved to a local reference for an easier estimation of the distances. Red solid lines depict the distances between the reference position and the receiver position at the same instant, while the blue ones the distances to the positions provided by our algorithm based on the Bancroft method. This image presents very well three typical cases in built-up areas. At the beginning

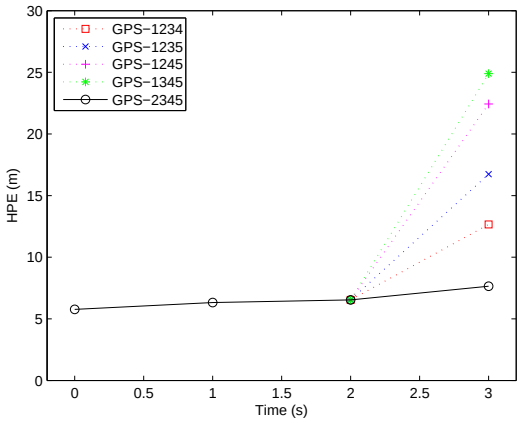

Fig. 6. Horizontal Positioning Error (HPE) during a period of 4 seconds. From t = 0 s till t = 2 s, the receiver detects only four satellites available (2–5). Therefore, there is only a possible combination and unique GPS solutions at each epoch during this period. At instant t = 3 s a new satellite (1) becomes available, resulting 5 satellites in view. The colored symbols (green $*$, magenta +, blue $\times$, red $\square$ and black $\circ$) identify the 5 different combinations of 4 satellites that lead to different positioning estimates.

of the test (the test vehicle moves from bottom-up and from right to left in the image) the NLOS detection method shows that all locked satellites were in line-of-sight. The receiver outputs are consequently good, and so they are the solutions obtained with our implementation of the Bancroft algorithm. Some meters ahead, even though the receiver keeps using all the satellites, our NLOS test detects that the visibility of a satellite has been blocked by one of the buildings on the right side of the road (labelled as 1 and 2 in the image). This satellite only appears visible at the antenna due to its reflection on building 3, 4 or 5 on the left side of the image. It is a clear example of NLOS multipath. Since the receiver was not aware of this, its solution is poor. However, our Bancroft solution is not affected by this outlier, showing consistency with the reference trajectory. After some other meters the satellite configuration changes again. This time, the rejection of NLOS satellites led to a bad geometry of the remaining satellites, causing poor DOP values. Due to the use of a space vehicle in NLOS, the receiver DOP value is good, although its position estimates wrong. In these cases, our method reports that with the current configuration is not feasible to estimate accurately the position of the vehicle.

Table III shows the statistical results for NLOS detection in terms of:

- Misdetection Rate (MDR) that represents those cases when there was a satellite in NLOS that was not reported.
- False Alarm Rate (FAR), that represents the cases

TABLE III
RESULTS OF THE NLOS DETECTION ALGORITHM.

MDR	FAR	OCDR	CMR	ECMR
0.0000	0.0207	0.9792	.09796	1.0000

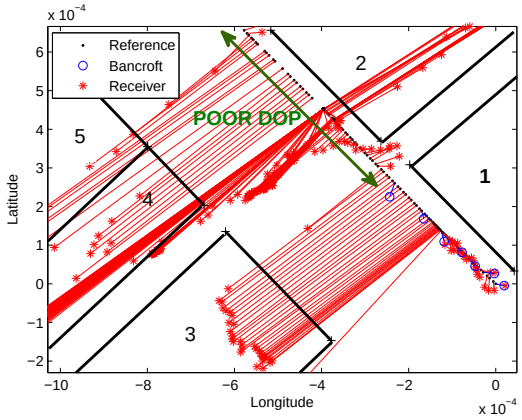

Fig. 7. Scenario with NLOS multipath.

when the method reports NLOS for one satellite that is actually in LOS,

- Overall Correct Detection Rate (OCDR), that can be calculated as OCDR = 1 – MDR – FAR.
- Correct Match Rate (CMR), that stands for the rate of correct NLOS detections and
- Enhanced Correct Match Rate (ECMR), that represents the addition of NLOS and LOS situations correctly identified.

Let us remind here that a DOP test is also performed before supplying a positioning solution with the remaining satellites. Let us also remark that the reference for NLOS detection was obtained by comparing the receiver pseudoranges with the real distances from the satellites to the reference DGPS post-processed position.

As it can be seen in Table III, the MDR is null, i.e. NLOS is never missed. On the contrary, a few false alarms appear as a consequence of the compensation carried out to cope with the EEMap data inaccuracies. The CMR is very high: in this test performed with 300 samples in an urban area, most of the samples included multipath effects, what brings even more the need of NLOS detection. Finally, the ECMR was just perfect.

The statistical analysis of the field tests is completed with the estimates of the Horizontal Positioning Error (HPE), shown in Table IV. Both positions, the one provided by the receiver in single mode and the one we estimate with the Bancroft algorithm after passing the aforementioned NLOS and DOP tests are compared. Only those samples that having at least 4 satellites in view show DOP values larger than 10 are computed. It is clear how the receiver fails at meeting the accuracy specifications due to multipath effects. However, our solution is fully consistent also in terms of HPE.

TABLE IV
HORIZONTAL POSITIONING ERROR.

	Mean	Std
Receiver	22.87	5.54
Bancroft	2.60	1.01

VI. CONCLUSIONS

The work presented in this paper aims at proving that a simple characterization of the vehicular environment can support the detection of faulty positions affected by multipath effects. To do it so, simple models of buildings were developed. The process of extraction of building features presented in the paper is relatively easy, flexible and fast. Highly precise, heavy and detailed models of buildings are disregarded in favor of light maps with only the most fundamental information. Among some other benefits, the proposed EEMap can be easily updated and downloaded where demanded.

Additionally, an algorithm that exploits the information stored in the EEMap to detect whether or not a satellite is in direct view was developed and introduced into the process of GPS positioning estimation. For that purpose, two GPS algorithms were developed and tested. The EEMap-based positioning algorithms were successfully applied in several field tests in scenarios with different features, proving the validity of our concept. Nevertheless, further tests are required before offering more detailed conclusions.

ACKNOWLEDGMENTS

The authors would like to thank Jose Santa, Miguel Ángel Zamora, Benito Úbeda and Pedro Pablo Martínez for their support in the test campaigns in Murcia.

REFERENCES

[1] GfK, “Portable satellite navigation systems on the road to success,” www.gfk.com/group/press information/press releases/002095/index. en.html, 2008.
[2] M. Tsakiri, M. Stewart, T. Forward, D. Sandison, and J. Walker, “Urban fleet monitoring with GPS and GLONASS”, The Journal of Navigation, vol. 51, pp. 382-393. Sep. 1998.
[3] F. Peyret “EGNOS-on-the-road: What Can Be Expected from EGNOS Compared to GPS for Road Traffic Management Services” In proc. of the ITS World Congress. PaperID: T-EU00897. Busan, Korea. 2010.
[4] M. Zabic, “Road Charging in Copenhagen: A Comparative Study of the GPS Performance,” 16th World Congress on Intelligent Transport Systems, Stockholm, Sweden, October 2009.
[5] O. Le Marchand, P. Bonnifait, J. Ibañez-Guzmán, F. Peyret, D. Bétaille, “Performance Evaluation of Fault Detection and Exclusion Algorithms as Applied to Automotive Localisation”, *In Proc. of the European Navigation Conference GNSS*, Toulouse, France, Apr. 2008.
[6] D. Betaille and R. Toledo-Moreo, “Creating Enhanced Maps for Lane-Level Vehicle Navigation,” IEEE Transactions on Intelligent Transportation Systems., vol. 11, no. 4, pp. 786-798, 2010.
[7] “Minimum Operational Performance Standards For Global Positioning System/Wide Area Augmentation System Airborne Equipment”. RTCA, RTCA/DO-229C Nov. 28, 2001 Supersedes DO-229B. 2001
[8] Cooperative Vehicle Infrastructure Systems. European Project of the 6th Framework Program. www.cvisproject.org
[9] R. Toledo-Moreo, David Bétaille, François Peyret, “Lane-Level Integrity Provision for Navigation and Map Matching With GNSS, Dead Reckoning, and Enhanced Maps”, IEEE Transactions on Intelligent Transportation Systems, vol. 11, No. 1, pp. 100–112, March 2010.
[10] John Canny. “A computational Approach to Edge Detection”. IEEE Transactions on Pattern Analysis and Machine Inteligence. Vol. 8. NO. 6, November 1986.
[11] G. Blewitt. “Basics of the GPS Technique: Observation Equations”. Department of Geomatics, University of Newcastle. Technical Report.
[12] S. Bancroft. “An algebraic solution of the GPS equations”. IEEE Transactions on Aerospace and Electronic System, Vol. AES-21, pp. 56-59. 1985.
[13] L. Harte, B. Levitan. “Global Positioning System (GPS)”. Althos books. ISBN: 1-932813-30-6. 2009.